DONNAN POTENTIALS IN RABBIT PSOAS MUSCLE IN RIGOR

G. R. S. NAYLOR, E. M. BARTELS, T. D. BRIDGMAN,* AND G. F. ELLIOTT
Biophysics Group, Open University, Oxford Research Unit, Boars Hill, Oxford, England

ABSTRACT Collins and Edwards (1971, *Am. J. Physiol.*, 221:1130–1133) have shown that a tissue potential can be measured with microelectrodes in glycerinated muscle and that this potential is consistent with a Donnan equilibrium of small ions due to the concentration of net fixed electric charge on the contractile proteins. This approach has been combined with x-ray and light diffraction measurements of the muscle lattice dimensions, and the data are used to determine the thick filament charge and thin filament charge under a variety of different conditions. The thick filament charge is a function of the bathing solution, in particular its pH and ionic composition. These parameters are important in determining the volume of the equilibrium lattice and possibly are involved in the contraction mechanism itself.

INTRODUCTION

The membrane system of striated muscle fibers can be disrupted by storing them in a 50% glycerol-water solution for several weeks at low temperatures (Szent-Gyorgyi, 1949, 1951). Most of the components of the sarcoplasm are leached out (Weber and Portzehl, 1952) but despite this comparatively rough treatment the structure of the contractile system is preserved as seen in the electron microscope (H. E. Huxley, 1957) and by x-ray diffraction (H. E. Huxley, 1953). Because of the absence of ATP the fibers are in rigor, but if they are bathed in a suitable solution containing ATP, they become relaxed and extensible, and if calcium is then added, they will contract and generate a tension similar to the maximum tension produced in live muscle (Weber and Portzehl, 1952, 1954). Thus glycerinated muscle is a simpler system than an intact fiber and is useful for the study of the basic contractile elements, avoiding the osmotic and ion-selective effects imposed by the fiber membrane.

Low-angle x-ray diffraction experiments (Rome, 1967, 1968; Matsubara and Elliott, 1972) in which the spacing of the thick filament lattice is measured in a variety of bathing media suggest that there are significant long-range electrostatic forces between the filaments (see also Elliott, 1967, 1968; Millman and Nickel, 1980). These long-range forces will depend upon the fixed charge on the protein filaments.

Naylor and Merrellees (1964) and Weiss et al. (1967) observed that a negative resting potential could be measured with microelectrodes in glycerinated fibers. Collins and Edwards (1971) showed that this tissue potential behaved as a Donnan phase boundary potential due to the net fixed electric charge on the contractile proteins.

We have considered elsewhere (Elliott and Bartels, 1982; Naylor, 1982) the way in which the measured potential is related to the point-to-point potential between the muscle filaments, and have demonstrated that in the practical regime the average potential can be considered as a simple Donnan average, so that the measured potentials can be used, together with the principle of electrical neutrality, to give the fixed electric charge on the contractile proteins. This is the calculation introduced by Collins and Edwards (1971) and used in its general form by Elliott et al. (1978).

Here the techniques of low-angle x-ray diffraction and electrophysiology are combined to determine the net fixed charge on the muscle filaments in situ. The overall aim is to characterize the net fixed charge for a variety of different conditions of the bathing medium and different physiological states of the muscle. Some preliminary results of this work have already been published (Elliott et al., 1978). The experimental techniques have since been modified, and it is shown that the preliminary results gave artifactually high values for the Donnan potential. Here results are presented for the A-bands of rigor fibers, in experiments varying the pH and ionic strength of the bathing medium. In the following paper the effects of relaxing solutions are considered in both A- and I-bands (Bartels and Elliott, 1985).

METHODS

Basis of the Method

Collins and Edwards (1971) demonstrated that the fixed charge concentration in muscle is due to the contractile proteins, since partial extraction of actin and myosin at high ionic strength reduced the measured potential (and thus the fixed charge concentration) without having any effect on the measured isoelectric point.

*Deceased.

Dr. Naylor's present address is Physics Department, James Cook University, Townsville, Q 4811, Australia.

To go one step further and measure the electric charge per filament, not just the charge concentration, it is necessary to determine the volume associated with the fixed charge, i.e., the volume occupied by each filament. Low-angle x-ray diffraction studies give the lattice spacing of the thick filaments and combining this with laser diffraction, which gives the sarcomere length, determines the volume of the sarcomere. Here specimens were examined by diffraction and microelectrode methods to give information on the actual filament charge rather than the charge concentration.

Specimen Preparation

Psoas muscle from several different rabbits were used for all the experiments. The method of glycerination was similar to that of Rome (1967), the glycerinating solution contained 50% glycerol (by volume) and 50% (by volume) 100 mM KCl, 2 mM $MgCl_2$, 4 mM EGTA, 7 mM KH_2PO_4, 13 mM K_2HPO_4, pH 7.0. Strips of muscle ~4 mm in diameter were stored in this solution for 2 d at 4°C, changing the solution every 8 h, and were then transferred to a freezer at −20°C for 3 wk before use.

Muscle strips were prepared at a wide range of sarcomere lengths by stretching the fresh muscle to different degrees before glycerination. For our sarcomere-length variation experiments specimens were chosen at several sarcomere lengths, measured by light diffraction (see below).

Small strips of muscle, ~1 mm in diameter and 30 mm long, were used in all experiments. They were left to soak in the required solution for 30 min before being transferred to the experimental cell and were then allowed another 30-min equilibration time. In many experiments the specimen was examined in several different solutions and a re-equilibration time of 30 min was found to be sufficient.

Bathing Medium

The standard salt solution used consisted of 100 mM KCl, 5 mM $MgCl_2$, 7 mM KH_2PO_4, 13 mM K_2HPO_4, pH 7.0. The ionic strength of the salt solution was varied by serial dilution of the standard solution to give a set of solutions with KCl contents 100, 50, 20, 10, and 5 mM. The free ion concentration of each species was calculated from the accumulative association constants of Sillén and Martell (1964) and Portzehl et al. (1964) with the computer program described by White and Thorson (1972) and Perrin and Sayce (1967). In experiments where the pH was varied a citric acid/K_2HPO_4 buffer was used from 3.5–6.0 pH; this is one of the few buffers that will act effectively over this range.

X-ray Diffraction

The first two equatorial diffraction maxima, the (1,0) and (1,1) reflections from the hexagonal lattice of myosin filaments were obtained using a modified double Franks camera (Elliott and Worthington, 1963) mounted on a fine-focus rotating anode x-ray generator (Elliott Automation GX-6 GC Avionic Ltd., Boreham Wood, United Kingdom). The camera was aligned to give a vertical line and a spot above it. A specimen to film distance of between 160 and 200 mm was used and measured to an accuracy of ±0.5 mm. An exposure time of 60–90 min gave well-defined patterns. Films were measured with a traveling microscope to an accuracy of 0.01 mm and thus a typical spacing of 40 nm could be determined to an accuracy of ±1 nm.

Light Diffraction

The sarcomere length was measured using light diffraction from a 0.5 mW helium-neon laser (λ = 0.6328 μm) with a beam ~1.5 mm in diameter. Because of specimen inhomogeniety the sarcomere length was determined to an accuracy of ±0.05 μm. Initially the same specimen was used for x-ray diffraction, laser diffraction, and microelectrode observation. Later, as more x-ray data were accumulated, it was found more convenient to make parallel x-ray and microelectrode observations on separate specimens from the same experimental batch, chosen at sarcomere lengths defined by laser diffraction. This change of procedure did not make any significant difference to the gradient of the pooled x-ray data plotted against sarcomere length.

Electrophysiology

Borosilicate glass capillary tubing with an inner fiber (Hildenberg, Glass, Malsfeld, Federal Republic of Germany) and of 1.5 mm outside diameter was used for the microelectrodes (Sato, 1977). It was possible to fill the microelectrodes completely by capillary action with a syringe (Tasaki et al., 1968); the microelectrodes were filled with 3 M KCl. A few microelectrodes were examined in the electron microscope (e.g., Fig. 1). The diameter range of the tips was 0.1–0.2 μm, for microelectrodes with a resistance of 25–30 MΩ. Microelectrodes were connected to a high impedance direct current (DC) amplifier (10^{14} Ω) via a silver-chloride junction (model EH-1S; Transidyne General Corp., Ann Arbor, MI) and the output was displayed on a suitable calibrated meter. The circuit was completed with a calomel reference electrode (Corning Glass Works, Corning Science Products, Corning, NY or Radiometer American Inc., Westlake, OH), and a variable millivolt source was available on the low impedance side for calibration. In each muscle sample, 20 potential readings were taken and averaged; a standard deviation was obtained, typically <1 mV.

Junction Potentials

The amplifier will see the phase potential between the muscle and the bathing fluid, added to two liquid potentials, one at the calomel electrode and one at the microelectrode. As long as these do not change on impalement they can simply be "backed-off." Kushmerick and Podolsky (1969) have shown that the ionic mobilities inside and outside the contractile lattice are unchanged, except for a "tortuosity" factor, which is the same for all ions. This will not affect the liquid junction potentials. Since the free ions are identical inside and outside the lattice, and the concentrations are similar, it is simple to show that the change in junction potential of the microelectrode will be ~0.1 mV, and can thus be disregarded.

In a recent abstract Rehm et al. (1984) have interpreted the potential seen with a 3 M KCl electrode impaling the corneal stroma (an analogous matrix of charged proteins and proteoglycans) as solely due to a junction or diffusion potential. They state that they "interpret the PD as due to the effect of fixed negative charges of connective tissue fibers on the ratio of the K^+ to Cl^- mobilities." However, it is the essence of a Donnan distribution that the local charge distribution is on the average neutral, both inside and outside the charged matrix, and it is difficult to believe that K^+ and Cl^- ions, diffusing out of the microelectrode tip, will be able to differentiate the charges on the matrix from those on the co- and counter-ions in local equilibrium with that matrix. The argument is thus physically implausible and is, moreover, in conflict with the experimental results of Kushmerick and Podolsky (1969) for muscle.

Rehm et al. (1984) and Davis et al. (1970) (and also Viera and Onuchic, 1978, for the stratum corneum) report that the potential measured with their microelectrodes was a function of the electrode filling solution, decreasing to zero when the concentration within the electrode was the same as the solution bathing the tissue. This is not evidence that changes in diffusion potentials are important, as can be seen using the formulation of Teorrell (1953), who considered a situation where two salt solutions were in equilibrium with opposite sides of an ionic membrane, which consisted of a fixed-charge matrix and an aqueous, salt-containing medium. Teorrell showed (Eq. 20:2) that sum of the Donnan potentials at the two surfaces could be expressed as

$$25.6\left(\sinh^{-1}\frac{\bar{X}}{2a_2}-\sinh^{-1}\frac{\bar{X}}{2a_1}\right)\text{mV}.$$

$\bar{X}$ is the concentration of fixed charge in the membrane (typically 50 mM) and a_1, a_2 are the salt concentrations on the first and second sides of the membrane. Taking the first side as the solution in the microelectrode and the second side as the bathing solution in experiments of the type made in

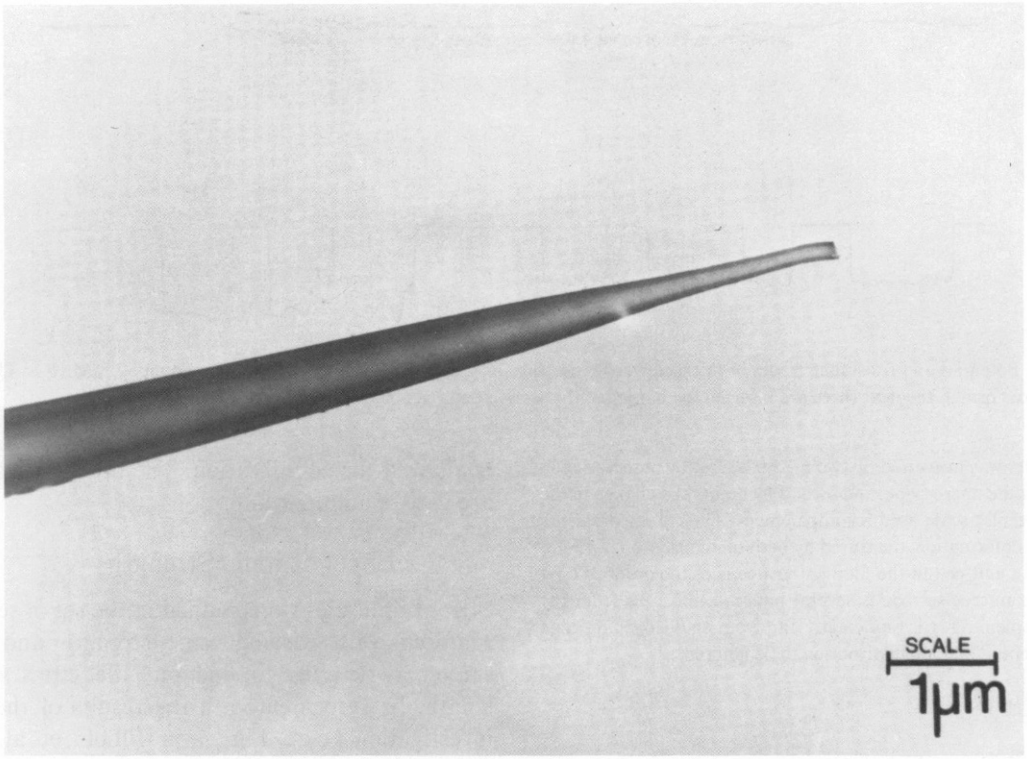

FIGURE 1 Electron micrograph of a typical microelectrode showing the tip diameter.

this paper and in the papers of Davis et al. (1970) and Viera and Onuchic (1978), it is easy to see that this sum will indeed be 0 if $a_1 = a_2$. It is also clear, though, that the second term is unimportant if $a_2 \sim 100$ mM and $a_1 \sim 3{,}000$ mM, which is the case in the experiments made in this paper. Under the conditions of these measurements, a typical experiment decreasing the salt concentration in the microelectrode gives, $E =$ (-9.3 ± 0.7)mV with 3 M KCl electrodes, (-9.4 ± 0.6)mV with 1 M KCl electrodes, and (-9.3 ± 0.6)mV with 0.5 M KCl electrodes.

Teorrell (1953) also considered a third component of potential, a diffusion potential between the two surfaces of the ionic membrane. This potential he expressed in Eq. 26:2, for the special case where a 1-1 valent salt is diffusing, as

$$25.6 \times \frac{u - v}{v + v} \ln \frac{a_1(r_1 u + v/r_1)}{a_2(r_2 u + v/r_2)} \text{mV}.$$

Here u,v are the mobilities of the diffusing cations and anions, respectively, and r_1,r_2 are the Donnan ratios at the first and second surfaces, which can be shown to be 1.00 and 0.78, for a fixed charge concentration of 50 mM, using Teorrell's Eq. 8:2. Apart from the extra terms in the brackets, this diffusion potential is the same in form as the conventional (Henderson) expression for the diffusion potential from an electrode containing a filling solution of concentration a_1 into a solution of concentration a_2. Taking the usual values for K^+ and Cl^- mobilities, the terms in the brackets give a modifying factor of 0.97 to the logarithmic term. The logarithm is 3.40 in the absence of this factor and 3.37 in its presence, so that the diffusion potential changes by ~1%, which underlines the statement made in the first paragraph under this subheading.

Tip Potentials

The tip of a microelectrode may also produce a potential of 10 mV or more, larger than that predicted from a liquid junction; this potential is called the "tip potential" of the microelectrode (Adrian, 1956). The tip potential depends on the tip diameter, the composition of the glass used, and the concentration, composition, and pH of the solutions both inside and surrounding the tip (Adrian, 1956; Kostyuk et al., 1968; Lavallee, 1964; Lev, 1968; Szabo, 1966). Adrian showed that the major determinants of changes in tip potential (which is the important factor in these experiments) were different ions in the solutions (i.e., going from a sodium-rich Ringer's solution to a potassium-rich cytoplasmic solution) and different concentrations of these ions. In the experiments described in this paper the ions are the same inside and outside the lattice, and the changes in concentrations are small, so that large changes in any tip potential would not be expected. Nevertheless the tip potential was routinely measured (compared to a broken and blunt microelectrode) and electrodes where this potential was >1 mV were discarded.

A resistance meter described elsewhere (Naylor, 1978) was added to the circuit to enable the resistance of the microelectrode to be monitored continuously during impalement. Schanne et al. (1968) showed that the resistance of the microelectrode changes at the same time as the tip potential. By monitoring the tip resistance during impalement, it is possible to avoid situations where the resistance changes dramatically due to partial blockage with a possible change in tip potential. Readings where the resistance varied by >10% were discarded as a matter of routine. It was found (see Results) that a yet more stringent test was needed, so high power light microscopy (Bartels and Elliott, 1981, 1982, and 1985) was used to observe the tip of the microelectrode during impalement. On some impalements where the resistance change was <10% some mechanical deformation of the tip was visible (e.g., a slight bending of the electrode). Careful examination revealed that these impalements gave artifactually high readings (Results, Fig. 2). Light microscopy was subsequently used routinely to avoid this artifact, and all the microelectrode experiments were repeated, giving smaller values for the averaged potentials than in the first report (Elliott et al., 1978).

Depth of Impalement

It is important that the electrode is far enough inside the lattice of filaments that edge effects are minimized. The depth of impalement of

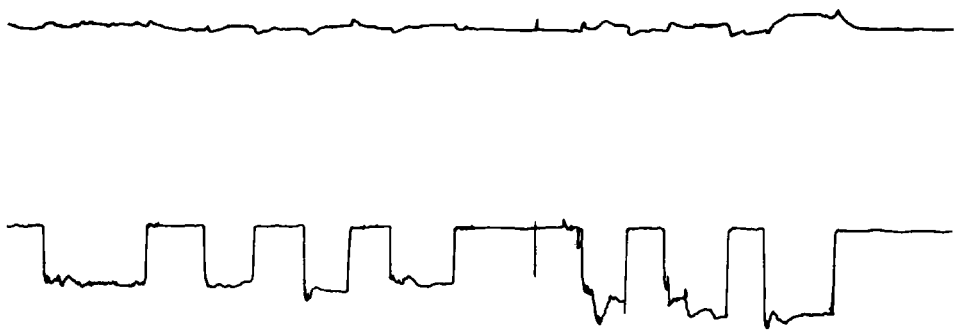

FIGURE 2 Potential and resistance traces of microelectrode insertions in a two-times diluted solution, based on 50 mM KCl. The first four insertions are normal, the next three are inserted too hard (see the section entitled Experiments in the Results).

the microelectrodes was measured by two methods, first by observation in the field of view of the microscope, and second by noting the change in the readings on the vernier scale used for impalement. Typical impalements without electrode deformation, measured by both methods, are 10–15 μm in depth. Since the unit cell in the filament lattice is of the order of 0.04 μm, the tip of the microelectrode is several hundred unit cells from the edge of the specimen. This is sufficiently far from that edge for edge effects on the potential and ion distribution to be ignored.

RESULTS

Initial Experiments

Fig. 2 shows a voltage and resistance trace of an experiment (made in a solution based on 50 mM KCl) under microscopic observation, which illustrates the problems with earlier data taken without microscopic observation. The first four impalements were made with the microelectrode seen in the microscope just to enter the A-band; the potential change is clear and apart from small transient changes, the resistance of the microelectrode does not vary outside the 10% previous criterion. The average of these impalements is about −7.5 mV. The next three impalements were made with a firmer touch on the micromanipulator. In the microscope the A-band could be seen to deform slightly, and in the last of these impalements the microelectrode could be seen to bend as impalement went deeper; these three readings are considerably higher than the earlier readings (average (~12 mV) and yet the resistance change of the microelectrode is still within the 10% criterion.

It seems clear that without microscopic observation of the electrode tip the observed potentials are higher than they would otherwise be and all the microelectrode experiments from the initial work have therefore been repeated. To see whether the history of a particular specimen would affect the measured potential or the measured x-ray spacing, it was necessary to study the effect of previous solutions on the specimen. (For example, when using several solutions is the order in which the solutions are used important?) These preliminary experiments were described in Naylor (1977). The conclusion was that the potentials and x-ray spacings measured are the same for a given specimen in a given solution as long as sufficient time is allowed for equilibration. The order in which solutions are used is unimportant.

Effect of Ionic Strength

Strips of muscles were studied in the set of serially diluted solutions with varying ionic strength and at different sarcomere lengths to find out the effect of sarcomere length. In agreement with the results of the preliminary investigation (e.g., Fig. 4 in Elliott et al., 1978), the observed potentials are independent of sarcomere length. Fig. 3 shows potential measurements plotted as a function of sarcomere length in four solutions of different ionic strength. The least-squares fit gradients of the straight lines, from the most concentrated to the most dilute solution in order, are −0.05, +0.34, +0.014, and −0.15 mV μm^{-1}. The largest gradient represents a change of only 0.48 mV over the range of lengths and this is within the standard deviation of the measurements. Since in addition these small gradients are two positive and two negative there is no consistent length effect, and the results from all sarcomere lengths have therefore been averaged in Table I. (See also the section entitled Absence of Sarcomere-Length Dependence: Further Details).

X-ray data were collected in the same solutions, giving the interfilament spacings $d(1,0)$ corresponding to the microelectrode data. A typical plot showing the variation of $d(1,0)$ as a function of sarcomere length for a particular solution is given in Fig. 4. As Rome (1967) observed, $d(1,0)$ and sarcomere length appear to be linearly related, with the spacing decreasing as the sarcomere is increased. The data were fitted to a straight line using a least-squares method and the equations so obtained are given in Table I.

Effect of pH

To study the effect of pH a set of four solutions was used — centered around the anticipated isoelectric point, pH = 4.5 (predicted from a minimum in the x-ray equatorial spacing [Rome, 1968] and a reversal in the sign of the Donnan potential [Collins and Edwards, 1971]). No x-ray pattern could be observed below pH = ~3.5, which was therefore chosen as the lowest pH. As far as possible one simple

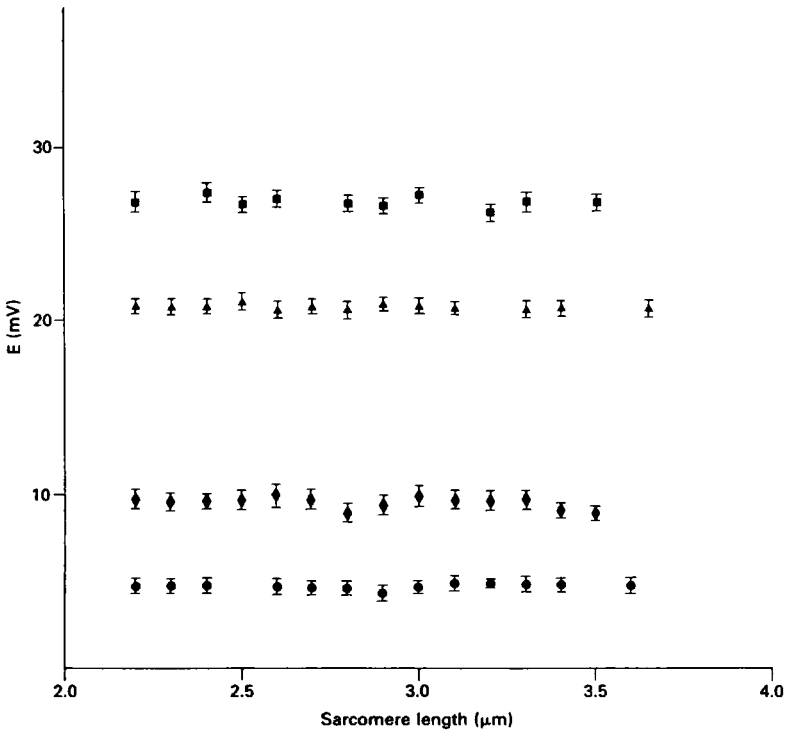

FIGURE 3 Potentials in four standard solutions, plotted as a function of sarcomere length. Circles, standard rigor solution; diamonds, two-times diluted triangles, five times diluted; squares, ten times diluted.

buffer system was used to avoid any possible effect of different binding affinities of different buffers to the filaments; a citric acid–K_2PO_4 buffer was chosen, allowing a maximum of pH 6.0. The data obtained at pH 7.0 in the previous section can be included with the results, though these were obtained with a different buffer system (phosphate) and may therefore not be strictly comparable.

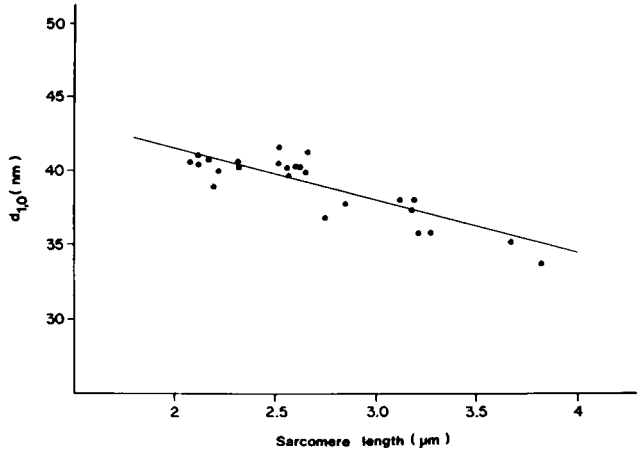

FIGURE 4 A plot of the x-ray spacing, $d_{1,0}$ as a function of sarcomere length S for the solution in the serial dilution set with [KCl] = 50 mM. The straight line shows the least-squares fit for all the data. Notice, however, that between S = 2.0 and ~2.6 μm there is no clear gradient in the observed data and only from S = 2.6–4 μm is there an appreciable change in side spacing (see Discussion, third paragraph).

pH Effect at Low Ionic Strength, [KCl] = 10 mM. Both x-ray and microelectrode techniques were used at a variety of different sarcomere lengths. Once again the potentials are independent of sarcomere length. The dependence of the potential changes sign and becomes positive, indicating a change in sign of the net electric charge on the filaments as shown in Fig. 5. This is effectively an in situ titration curve, and gives an isoelectric point of pH 4.5.

A summary of the corresponding x-ray data is also given in Table II, A. At the three higher pH's the x-ray lattice spacings decrease with decreasing pH but the least-squares straight lines for pH = 3.5 and pH = 4.0 intersect so that at short sarcomere lengths the spacing continues to decrease, whereas at long sarcomere lengths a minimum is observed. These results agree well with Rome (1968) who found a minimum spacing at pH 4.7 for long sarcomere length data (S = 3.15 μm) but observed no minimum spacing at short sarcomere lengths. Thus the pH behavior of the spacing of the myosin lattice unperturbed by the actin (at long sarcomere length) appears to reflect directly the charge on the thick filaments.

pH Effect at High Ionic Strength [KCl] = 50 mM. To see the effect of ionic strength on the titration curve and the isoelectric point the experiment was repeated at a higher ionic strength. The potentials were again independent of sarcomere length and the average potentials are also plotted as a function of pH in Fig. 5. This

TABLE I
SUMMARY OF RESULTS OF VARIATION OF IONIC STRENGTH

Solution	E	[Pr]	X-ray data	σ_m/σ_a	σ_m	σ_a
	mV	*mM*			*e/nm*	*e/nm*
100 mM KCl 5 mM $MgCl_2$ 20 mM phosphate buffer pH 7.0 μ = 0.14M	−4.7 ± 0.6 *n* = 400	52 ± 7	*d** = (47.2 ± 1.6) −(3.0 ± 0.5) × *S*‡ *n* = 31	7.1	47	6.5
2 × dilution, 50 mM KCl, etc. μ = 0.071 M	−9.7 ± 1.1 *n* = 400	56 ± 7	*d* = (48.1 ± 1.1) −(3.4 ± 0.5) × *S* *n* = 43	6.1	45	7.4
5 × dilution, 20 mM KCl, etc. μ = 0.029 M	−20.8 ± 1.1 *n* = 400	56 ± 4	*d* = (56.1 ± 1.5) −(6.3 ± 1.2) × *S* *n* = 28	2.7	40	15
10 × dilution, 10 mM KCl, etc. μ = 0.015 M	−26.8 ± 1.2 *n* = 400	40 ± 3	*d* = (59.6 ± 1.8) −(7.0 ± 1.5) × *S* *n* = 21	2.5	30	12
20 × dilution, 5 mM KCl, etc. μ = 0.0074 M	−34.6 ± 1.8 *n* = 40	31 ± 3	*d* = (68.9 ± 2.0) −(9.6 ± 2.7) × *S* *n* = 14	1.7	22	13

σ_m and σ_a are the linear densities, the thick and thin filaments, respectively. All potentials and the associated [Pr] are given as a mean and standard deviation. The x-ray data are shown as the least-squares straight line fit to the experimental data, with standard errors calculated in the normal manner. The charge ratios in column 5 have a precision of about ±50%, the thick filament linear charge in column 6 of about ±25%, and the thin filament linear charge in column 7 (much less precise for reasons given in the text; see Analysis) of about ±75%.

**d* is measured in nanometers.

‡*S* is measured in microns.

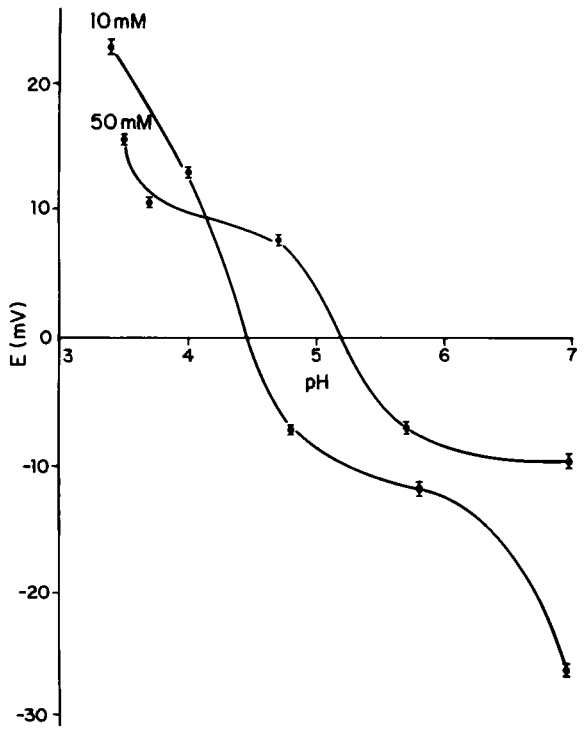

FIGURE 5 A plot showing the variation of the Donnan potential *E* as a function of pH. (*a*) [KCl] = 10 mM (*b*) [KCl] = 50 mM. The error bars show the standard error of the mean. Note that the measurements at pH 7 were obtained with a different buffer (phosphate) and may not therefore be strictly comparable with the other points, in citrate buffer.

shows an isoelectric point of pH = 5.2, so that the in situ isoelectric point has shifted to a higher pH on increasing the ionic strength. The corresponding x-ray data are also summarized in Table II, B. At pH = 6.0 and 5.0 the dependence of the $d(1,0)$ spacing on sarcomere length is less pronounced than in the low ionic strength solution.

Absence of Sarcomere-Length Dependence: Further Details

We have made extensive investigations of the measured potentials at different sarcomere lengths in an attempt to discover any sarcomere length dependence of the potentials. In no case was such an effect observed either in rigor solutions of different ionic strength (Elliott et al., 1978), rigor solutions of different pHs, or of different magnesium concentrations, or in relaxing solutions (Naylor, 1977; Bartels and Elliott, 1985), and the measured potentials are independent of sarcomere length in all the solutions that have been investigated.

In the preliminary experiments (Elliott et al., 1978) it had been concluded that in rigor muscle there were different charge concentrations in the A-bands and I-bands and therefore there should be different potentials arising from those bands. It therefore seemed possible that two families of potentials might be seen at longer sarcomere lengths, when the chance of hitting an I-band ought to be greater. Accordingly, a series of observations were made without light microscopy, recording large numbers (~150)

TABLE II
SUMMARY OF RESULTS OF VARIATION OF pH VARIATION

Solution	E	[Pr]	X-ray data	σ_m/σ_a	σ_m	σ_a
A.	*mV*	*mM*			*e/nm*	*e/nm*
10 mM KCl	−11.8 ± 0.8	−11 ± 1	d^* = (55.4 ± 2.0)	2.3	7	3
0.5 mM $MgCl_2$			−(6.4 ± 1.6) × S‡			
0.8 mM phosphate/citric-acid buffer						
pH 5.8						
μ = 0.013 M	n = 100		n = 17			
As above	−7.2 ± 0.5	−6 ± 1	d = (50.6 ± 2.2)	3.6	4	1.1
pH 4.8			−(5.0 ± 1.2) × S			
μ = 0.014 M	n = 100		n = 18			
As above	12.9 ± 0.7	14 ± 1	d = (49.2 ± 1.8)	2.5	7	2.8
pH 3.95			−(5.7 ± 1.4) × S		net positive charge	net positive charge
μ = 0.014 M	n = 100		n = 17			
As above	22.7 ± 0.7	27 ± 1	d = (32.3 ± 1.7)	−42	21	0.5
pH 3.4			+(0.5 ± 0.05) × S		net positive charge	
μ = 0.014 M	n = 100		n = 14			
B.						
50 mM KCl	−7.1 ± 0.5	−32 ± 3	d = (38.5 ± 1.6)	32.2	29	0.9
2.5 mM $MgCl_2$			−(0.6 ± 0.1) × S			
4 mM phosphate/citric-acid buffer						
pH 5.7						
μ = 0.071 M	n = 100		n = 19			
As above	7.5 ± 0.8	42 ± 5	d = (36.9 ± 1.4)	25.9	33	1.3
pH 4.7			−(0.8 ± 0.2) × S		net positive charge	net positive charge
μ = 0.069 M	n = 100		n = 20			
As above	10.6 ± 0.7	60 ± 4	d = (34.6 ± 1.4)	30.5	58	1.9
pH 3.7			−(0.9 ± 0.2) × S		net positive charge	net positive charge
μ = 0.071 M	n = 100		n = 17			
As above	15.5 ± 0.6	92 ± 4	d = (33.7 ± 1.3)	73.3	66	0.9
pH 3.5			−(0.5 ± 0.03) × S		net positive charge	net positive charge
μ = 0.073 M	n = 100		n = 18			

*d is measured in nanometers.
‡S is measured in microns.

of potentials observed by random penetration in preparations at a range of sarcomere lengths in the rigor solution based on 20 mM KCl (fivefold dilution) and plotting the results in the form of histograms. These are shown in Fig. 6 *a–d*). It will be seen that at the longer sarcomere lengths (3.0 and 3.3 μm) the distribution is skewed at the lower potential end, while at the shortest sarcomere length (2.2 μm) the histogram shows a more nearly symmetrical distribution. It was not possible, however, to distinguish two separate peaks in experiments of this type with glycerinated rabbit muscle at long sarcomere lengths. The best-fit Gaussian curves are also seen in Fig. 6 *a–d*, and it will readily be appreciated that the mean potentials did not vary outside the experimental error, as was apparent also from the other experiments. Notice that the skewing of the histograms in Fig. 6 is not due to a sarcomere length effect on the A-band potential, which is eliminated by the data shown in Fig. 3. It is the result of the convolution of the A-band potential with the I-band potential, which is more likely to be observed in random observations at long sarcomere length. In experiments under optical control, where the location of the electrode is known, the data are not skewed in this manner.

It seems, therefore, that random penetration experiments, made without light microscope back-up, record the A-band potential in glycerinated rabbit muscle. In the subsequent paper further observations relevant to this point will be reported.

What Is the Effect of the H-Zone?

Although there is, in rigor glycerinated rabbit psoas muscle, a clear difference between the observed A- and I-band potentials (Bartels and Elliott, 1981, 1985) no effect has been seen experimentally in these muscles that needs be assigned to a manifestation of different potential regions in the overlap region of thick and thin filaments and in the H-zone of nonoverlap at the center of the A-band. Now there clearly is a different potential regime in the overlap and nonoverlap regions of the A-band, and if the experi-

EACH X = 0.33 PERCENT
EACH X = 0.33 PERCENT
EACH X = 0.26 PERCENT
EACH X = 0.26 PERCENT
a
b
c
d

mental method were sufficiently sensitive, it might be possible to detect the Donnan effects of these two different potential regions. This has not been observed here, nor has it been observed in the experiments of Aldoroty and April (1984) and Aldoroty et al. (1985) who have made similar measurements on crayfish muscle, where the A-band is three times longer than in rabbit or rat and where it therefore would be easier to detect the H-zone region when placing the microelectrode.

A possible reason for this inability to detect different H-zone potential is that the region over which the microelectrode senses an average is of the order of a 1-μm diameter sphere. This would tend to average both H-zone and overlap zone in an A-band of 1.6 μm in length. Whatever may be the reason, Fig. 3 shows that there is no sarcomere length on the observed A-band potential, as might have been expected from an H-zone effect.

ANALYSIS

The concentration of all ions in the external solution can be calculated from the Perrin program. Therefore, when the Donnan potential has been determined, the application of the Nernst equation gives the concentrations of all these diffusible ions inside the filament lattice. Since the lattice must maintain electrical neutrality, the protein charge concentration [Pr^-] in millimolar units is given by: $[Pr] = \Sigma c_i^+ z_i^+ - \Sigma c_i^- z_i^-$, where c_i^+ and z_i^+ are the internal millimolar concentrations and valencies of the diffusible cations and c_i^- and z_i^- are the internal concentrations and valencies of the diffusible anions. Normally, with a negative Donnan potential this equation expresses the concentration of net negative charge on the protein filaments. Since the concentrations are all expressed in millimolar quantities it is simplest to express [Pr] in millimoles of univalent charge, because the valency of the charged matrix is unknown.

The working hypothesis for the interpretation of the preliminary results was that a microelectrode inserted randomly in glycerinated muscle in rigor recorded the higher A-band potential rather than the lower I-band potential (Elliott et al., 1978). Experimentally, this A-band potentials is indepedent of sarcomere length. In the present experiments microelectrode measurements have been combined with direct observation of the microelectrode tip under a high-powered light microscope and under these circumstances it is possible to differentiate between A- and I-band potentials, see Bartels and Elliott (1985).

Using the A-band potential alone, however, combined with the x-ray data, it is possible to calculate the charge on the thick and thin filaments. At long sarcomere lengths the A-band is composed solely of thick filaments, and one unit cell contains exactly one thick filament. Thus σ_m, the net charge on the thick filament (per unit length) is given by: σ_m = [Pr] × (volume occupied by unit length of the filament) × N_o, where N_o is Avogaradro's number. But volume occupied by the filament per unit length is $d_{3,8}^2/\sin 60°$. (Adopting the notation $d_{3,8}^2$ for the square of the value of d[1,0] evaluated at S = 3.8 μm). Hence $\sigma_m = 6.95 \times 10^{-4} \times [Pr] \times d_{3,8}^2$. It is assumed that the myosin filaments are 1.6 μm in length and the actin filaments are 1.1 μm in length, reasonable values for mammalian muscle, so that 3.8 μm is the point of zero overlap. If d is nanometers, and [Pr] is millimolar, σ_m is in electrons per nanometer.

At the short sarcomere length (S = 2.2 μm), where the thin filaments just meet, a unit cell in the A-band contains exactly one thick filament and two thin filaments. Thus the net charge (per unit length) on the thin filament σ_a is given by: $2\sigma_a + \sigma_m = 6.95 \times 10^{-4} \times [Pr] \times d_{2,2}^2$ (where $d_{2,2}^2$ is the square of the value of d[1,0], evaluated at S = 2.2 μm). Combining this expression with the expression evaluated above for σ_m, $\sigma_a = 3.48 \times 10^{-4} \times [Pr] \times (d_{2,2}^2 - d_{3,8}^2)$ and the charge ratio, $\sigma_m/\sigma_a = 2\, d_{3,8}^2/(d_{2,2}^2 - d_{3,8}^2)$. Notice that this ratio does not depend on the value of [Pr], and thus of the value of the measured potential, but only on the parameters of the x-ray data. It does depend on the experimental fact that the A-band potential is independent of the sarcomere length, and thus that the A-band charge concentration is the same at all sarcomere lengths (see also Elliott, 1973).

σ_a and σ_m are given in Table I for the experiments varying ionic strength and in Table II for the experiments varying pH. In the calculations we used the values for the spacings d(1,0) that are predicted from the least-squares fit. The values calculated for σ_a are inherently of low precision because of the subtraction of two large and nearly equal numbers, $d_{2,2}^2$ and $d_{3,8}^2$.

DISCUSSION

Veracity of the Method

The electrophysiology of the Donnan potential measurements has been discussed by Elliott and Bartels (1982) and in the Methods section here. Two additional points may be made.

(*a*) First, Aldoroty and April (1984) have performed elegant model experiments using agar gels, and have shown that the measured Donnan potentials behaved as expected when the concentration of the agar was varied. In other experiments the potential was unchanged when the tip diamenter was varied, when the concentration of KCl in the electrode was varied, and when the bathing solution was changed from potassium chloride to the same concentration of potassium propionate. They report that the absence of significant variation under these conditions, where diffusion potentials would be expected to change,

FIGURE 6 Histograms of a large number (150+) of potential readings taken in the same solution (the five times diluted solution based on 20 mM KCl) at different sarcomere lengths (*a*) 2.2 μm, (*b*) 2.6 μm, (*c*) 3.0 μm, and (*d*) 3.3 μm.

demonstrates that artifactual diffusion potentials do not contribute significantly to the measurements. (*b*) Second, the A-band of a rabbit muscle fiber contains proteins whose amino-acid sequence data are known, and whose charge can therefore be calculated (Appendix). At zero overlap none of the thin filament proteins contribute to the A-band charge. The volume can be measured with precision by a combination of x-ray and light diffraction. Under low ionic strength conditions, where ion binding would be expected to be minimal, the measured thick filament charge by the methods used here is 22 electrons (e) nm^{-1}. The calculated charge range (Appendix) is 9–26 e nm^{-1} (depending on the degree of ionization of the histidine residues) with a mean at ~ 18 e nm^{-1}. The accord between these two values is pleasing, and gives added confidence in the veracity of the method.

Discussion of the Experimental Results

The approximate linear behavior of the x-ray lattice spacing as a function of sarcomere length is similar to that observed by Rome (1967, 1978). In Rome's study of the effect of ionic strength the results are in good agreement with ours at short sarcomere length; at long sarcomere lengths (3.2 μm) she found that the spacing decreased with increasing dilution (opposite to the effect at short sarcomere length, S = 2.9 μm). This effect was not observed in our experiments at S = 3.2 μm but is clearly seen at S = 3.8 μm (i.e., at zero overlap). Thus at long sarcomere lengths the behavior of the lattice spacing in the myosin lattice unperturbed by actin filaments follows the electric charge on myosin (see Table I). Compare this with the similar pH behavior (see Results).

(In collaboration with Professor B. M. Millman of Guelph University [Guelph, Canada] a computer data bank has been established of all the available published and unpublished x-ray equatorial data on muscle, collected by several different investigators, in several different laboratories, over the last two and a half decades. The least-squares fit straight lines of the x-ray data in Table I agree closely with the collations of all this data. This is particularly true for the 100-mM solution, where the data bank contains a total of 226 individual observations.)

We are aware that it is only approximately correct to treat the x-ray data as a linear function of sarcomere length, and that the experiments of Shapiro et al. (1979) and Magid and Reedy (1980) show nonlinear behavior. (Indeed some of the present x-ray data show similar nonlinearity, see Fig. 4.) For the present purposes however, the precision of this approximation is sufficient for the analysis presented.

The trend of our observations of potential as a function of ionic strength agrees with that of Collins and Edwards (1971) who studied glycerinated frog ventricle and sartorius, and found that the fixed charge concentration increased with [KCl]. The major result of these experiments is that the net charge on the thick filament varies considerably with ionic strength, even taking into account the volume changes due to the swelling of the lattice. The thin filament charge, in comparison (although its determination is less accurate) seems to be less dependent on the ionic composition of bathing solution.

There are two effects that might account for the variation in the thick filament charge.

(*a*) First, hydrogen ions themselves will be distributed across the phase boundary according to the Donnan equilibrium and thus the pH of the medium surrounding the filaments will not be the same in the various solutions. For the experiment varying the total ionic strength the internal pH varies from 6.8 to 6.2, the lower ionic strength giving the higher internal pH.

At this point the effect of the changing internal pH on the thick filament charge will be considered in more detail. It is well known that the range pH 6–7 probably contains the effective pK of the histidine residues in proteins. Fig. 5 shows that there are definite changes in potential over this range of pH and there must be a similar change in fixed charge also. Is this sufficient to account for the effects seen in Table I? It is shown in the Appendix that there are 82 histidine residues on myosin and its associated light chains. If all these histidine residues became ionized the myosin filament charge would decrease from 26–9 e nm^{-2} (Appendix). The measured values lie from 47–22 e/nm. Put in another way, the change in myosin charge concentration would be less than the existing amount, i.e., 12 mM (Appendix), and the observed change is from 56–30 mM. The histidine effect seems insufficient to account for this even if allowance is made for a change of the actin charge to take account of its histidine content, 8 per monomer from the data of Collins and Elzinga (1975). (Tropomyosin and the troponins have negligible amounts of histidine according to the sequence data mentioned in the Appendix.) It is interesting though that on the interpretation given here the thick filaments, which contain the larger amount of histidine per unit length, are also those that seem to have ion-binding properties (see *b* below) and it might be speculated that one effect may perhaps be involved in the other.

(*b*) Second, the effect of ion binding must be considered. The major effect is due to the binding of a negative ion since on dilution the binding is presumably reduced and it is seen experimentally that the negative charge is reduced. There are therefore three possibilities for this binding, either chloride ions or phosphate ions or both of these ions together. The present experiments do not distinguish between these possibilities, although note that the chloride ions are present at much higher concentrations. In other experiments, to be reported in a subsequent paper (Bridgman, T. D., E. M. Bartels, and G. F. Elliott, manuscript in preparation; see also Elliott, 1980), it has been shown that either chloride or phosphate in the absence of the other is sufficient for this effect, that both appear able to bind at the same time, but that the binding of phosphate ions is interactive with the level of free magnesium ions, so that an increase of the magnesium causes a fall in Donnan poten-

tial, and therefore of protein charge concentration, if there are phosphate ions present.

The term ion binding is used here to refer to ions that are associated with the fixed-charge matrix of the total system and are thus not freely diffusible in and out of the system. This does not imply that these are necessarily covalently bound. Probably they are associated electrostatically with the matrix, and possibly it would be better to use the older term adsorbed ions.

In the Appendix expected thick and thin filament charges have been calculated on the basis of sequence data for the contractile proteins. The measured values for the thin filament charge, in the range 6–15 e nm^{-1}, agree well with the calculated value considering that the error of measurement is large. The measured values for the thick filament charge are up to two and a half-times the calculated value, though they drop to the calculated value as the ion concentration approaches zero, Table II. It is this fact that leads to the postulation of negative ion binding as an important characteristic of intact thick filaments in glycerinated psoas muscle. The total of all the calculated charge concentrations is <30 mM, the measured values range from 30–60 mM, and increase with ionic strength. This strongly suggests that negative ion binding must occur somewhere in the contractile system. Moreover the same conclusion can be drawn from the data of Collins and Edwards (1971) and Pemrick and Edwards (1974) if their values of charge concentration are recalculated using all the ions in their solutions and not just the KCl concentrations as they have done.

The experiments varying the pH of the bathing solution confirm and extend the earlier results of Collins and Edwards (1971) who showed a reversal in the sign of the measured potential at low pH. The data also confirm the x-ray results of Rome (1968), i.e., that the interfilament spacing decreases with decreasing pH and that at long sarcomere lengths there is a distinct minimum of the interfilament spacing at low pH. The fact that the potential changes sign at this point is very strong evidence that the potential being measured is related to the Donnan potential since it follows the sign of the net charge on the filaments, changing on passing through the isoelectric point. The graph of the potential vs. the pH represents the titration curve of the proteins, probably essentially the titration curve of the thick filaments because the A-band at long sarcomere lengths is composed solely of thick filaments, which contain mainly myosin but also a small amount of other components, notably C-protein (Offer, 1973). The change is slope of the curves near pH 7.0 is in the histidine *pK* region, which appears to depend on the ionic strength.

The experimental data have been analyzed on the hypothesis that the measured potential is a Donnan potential, and is the average of the potential well between the filaments (see Elliott and Bartels, 1982; Naylor, 1982). This hypothesis has been substantiated by previous workers (Collins and Edwards, 1971; Pemrick and Edwards, 1974), who showed that the potential increased on decreasing the ionic strength and behaved in the expected manner on different sides of the isoelectric point of the muscle proteins. These experiments have been repeated and extended with a similar outcome and there seems to be no difference between the behavior of the experimental tissues. Using this hypothesis a detailed analysis of the data yields a self-consistent set of results that are in agreement with other data. In this respect the experiments varying pH are important; these results show that the titration curve and the isoelectric point of myosin are a function of the ionic composition of the bathing medium.

APPENDIX

Charge Values from Sequence Data

The data of Barlow and Thornton (1983, and personal communication) established that at least 85% of the ion-pairs in known protein structures are accessible to the solvent, and that the unpaired ionic groups are also so accessible. Rashin and Honig (1984) put the proportion even higher, >95%. It is therefore reasonable to predict the net protein charge on any protein from the amino acid or sequence data.

Such an attempt to predict filament charges, and hence muscle charge concentration was made by Elliott (1973). The major problem at that time was that the amide NH_3 is difficult to measure with accuracy and had largely been left unmeasured by workers more recent than Kominz et al. (1954). A secondary problem was that the number of myosin molecules in a myosin filament was a matter of controversy. Using a myosin charge value of 15 electrons per 10^5 daltons (or ~75 e for the whole molecule) from Kominz et al. (1954), which agreed with the titration data of Milhayi (1950), Elliott (1973) calculated a thick filament charge of ~20 e nm^{-1}. (This calculation assumed Huxley's [1960] figure of 432 myosin molecules per filament.) Pepe's (1967) model for the myosin filament has ~400 molecules, similar to Huxley's number, so that the calculated filament charge using Pepe's model does not differ appreciably from Elliott's calculation. Squire's (1973) model has ~300 molecules, giving a figure of ~15 e nm^{-1}. These filament-charge figures ignored the C-protein (Offer, 1973) but this is unlikely to cause more than a 10% error. They also ignored the myosin light chains, see below.

The recent complete myosin sequence data of McLachlan and Karn (1982) and Karn et al. (1983) for nematode myosin, gives 90 e/molecule of which 94 e is on the myosin rod and 2 e^+ on each myosin head. Each myosin molecule in rabbit fast muscle has four light chains associated with it, two to each myosin head, and the sequence data on these are given by Grand (1982). These add 19 e to each myosin head, making a total charge on myosin heavy and light chains of 128 e. (Notice in passing that the light-chain charge makes a considerable difference to the myosin head charge, as might be appropriate for a control function. Equal occupancy of LC_1 and LC_3 has been assumed).

In these calculations it has been assumed that none of the histidine residues are ionized at physiological pH. There are a total of 82 histidine residues on the molecule and its light chains (34 on the rod, 21 on each head, and 3 on the light chains associated with each head). If all these were ionized the 128 e would fall to 46 e.

It is now clear that the myosin filament is three stranded (Kensler and Stewart, 1983) so that there are 300 myosin molecules in a rabbit or frog thick filament. The total range for the myosin filament charge from amino acid sequence and structural data is thus 9–26 e nm^{-1}, a rather wide range that includes the 1973 estimate. Taking the average value ~18 e nm^{-1}, and a sarcomere volume at $S = 3.8$ μm of 4×10^{-15} ml in the solution with 100 mM KCl (from the data given in Table I), the charge concentration in the whole sarcomere due to the myosin filaments is ~12 mM, which is close to the value (12.1 mM) given by Pemrick and

Edwards (1974) who approached the same problem from bulk protein-concentration measurements.

For the thin filaments, Elliott (1973) calculated ~10 e nm^{-1}. This also can now be modified since the actin sequence data of Collins and Elzinga (1975) give a precise figure, 7 e, for the actin molecule charge, the tropomyosin sequence data of Stone and Smillie (1978) gives 50 e for tropomyosin, the sequence data of Collins et al. (1977) for troponin C gives 29 e for that protein, the sequence data of Pearlstone et al. (1977) gives 9 e^+ for troponin T and the sequence data of Wilkinson and Grand (1975) gives 9 e^+ for troponin I. The total net molecular charge on the troponins is thus 11 e (negative). From these figures the thin filament charge is 2.5 e nm^{-1} due to actin, 2.4 e nm^{-1} due to tropomyosin, and 0.5 e nm^{-1} due to the troponins, and the total calculated thin filament charge is 5.4 e μm^{-1}. The charge concentration in the whole sarcomere due to actin is 4.6 mM, considerably less than Pemrick and Edwards (1974) figure (19.2 mM); this is due to their using an actin charge (24 e) that is untenable in the light of the sequence data. The other values (4.4 mM due to tropomyosin and 5.7 due to the troponins) are not appreciably different from those given by Pemrick and Edwards (1974).

We are grateful to Professor B. M. Millman and Drs. Tony Angel, Charles Edwards, David Gayton, Suzanne Pemrick, Mark Shoenberg, and Tony Woolgar for help, advice, and useful discussions during the course of this work.

We would particularly like to acknowledge the students of the Open University course S321, "The physiology of cells and organisms," whose work on experiments of this type over eight years in successive summer schools has shown us the reality of the phenomena that we observe.

Received for publication 28 March 1984 and in final form 19 November 1984.

REFERENCES

Adrian, R. H. 1956. The effect of internal and external potassium concentration on the membrane potential of frog muscle. *J. Physiol. (Lond.)*. 133:631–658.

Aldoroty, R. A., and E. W. April. 1984. Donnan potentials from striated muscle liquid crystals. A-band and I-band measurements. *Biophys. J.* 46:769–779.

Aldoroty, R. A., N. B. Garty, and E. W. April. 1985. Donnan potentials from striated muscle liquid crystals. Sarcomere length dependence. *Biophys. J.* 47:89–96.

Barlow, D. J., and J. M. Thornton. 1983. Ion-pairs in proteins. *J. Mol. Biol.* 168:867–885.

Bartels, E. M., and G. F. Elliott. 1981. Donnan potentials from the A- and I-bands of skeletal muscle, relaxed and in rigor. *J. Physiol. (Lond.)*. 317:85–87P.

Bartels, E. M., and G. F. Elliott. 1982. Donnan potentials in rat muscle: difference between skinning and glycerination. *J. Physiol. (Lond.)*. 327:72–73P.

Bartels, E. M., and G. F. Elliott. 1985. Donnan potentials from the A- and the I-bands of glycerinated and chemically skinned muscles, relaxed and in rigor. *Biophys. J.* 48:61–76.

Collins, E. W., and C. Edwards. 1971. Role of Donnan equilibrium in the resting potentials in glycerol-extracted muscle. *Am. J. Physiol.* 221:1130–1133.

Collins, J. H., and M. Elzinga. 1975. The primary structure of actin from rabbit skeletal muscle. *J. Biol. Chem.* 250:5915–5920.

Collins, J. H., M. L. Greaser, J. D. Potter, and M. J. Horn. 1977. Determination of the amino acid sequence of troponin C from rabbit skeletal muscle. *J. Biol. Chem.* 252:6356–6362.

Davis, T. L., J. W. Jackson, B. E. Day, R. L. Shoemaker, and W. S. Refrew. 1970. Potentials in frog cornea and microelectrode artefact. *Am. J. Physiol.* 219:178–183.

Elliott, G. F. 1967. Variations of the contractile apparatus in smooth and striated muscle. *J. Gen. Physiol.* 50 (Pt. 2):171–184.

Elliott, G. F. 1968. Force-balances and stability in hexagonally-packed polyelectrolyte systems. *J. Theor. Biol.* 21:71–87.

Elliott, G. F. 1973. Donnan and osmotic effects in muscle fibers without membranes. *J. Mechanochem. Cell Motil.* 2:83–89.

Elliott, G. F., and E. M. Bartels. 1982. Donnan potential measurements in extended hexagonal polyelectrolyte gels such as muscle. *Biophys. J.* 38:195–199.

Elliott, G. F., and C. R. Worthington. 1963. A small-angle optically focusing x-ray diffraction camera in biological research. Part I. *J. Ultrastruct. Reson.* 9:166–170.

Elliott, G. F., G. R. S. Naylor, and A. E. Woolgar. 1978. Measurements of the electric charge on the contractile proteins in glycerinated rabbit psoas using microelectrode and diffraction effects. *In* Ions in Macromolecular and Biological Systems. (Colston Papers No. 29). D. H. Everett and B. Vincent, editors. Scientechnica Press, Bristol, United Kingdom. 329–339.

Grand, R. J. A. 1982. The structure and function of myosin light chains. *Life Chem. Rep.* 1:105–160.

Huxley, H. E. 1953. X-ray analysis and the problem of muscle. *Proc. R. Soc. Lond. B. Biol. Sci.* 141:59–62.

Huxley, H. E. 1957. The double array of filaments in cross-striated muscle. *J. Biophys. Biochem. Cytol.* 3:631–648.

Huxley, H. E. 1960. Muscle cells. *In* The Cell. J. Brachet and A. E. Mirsky, editors. Academic Press, Inc., New York. 365–481.

Karn, J., S. Brenner, and L. Barnett. 1983. Protein structural domains in the *Caenorhabditis elegans unc*-54 myosin heavy gene chain are not separated by introns. *Proc. Natl. Acad. Sci. USA.* 80:4253–4257.

Kensler, R. W., and M. Stewart. 1983. Frog skeletal muscle thick filaments are three-stranded. *J. Cell. Biol.* 96:1797–1802.

Kominz, D. R., A. Hough, P. Symonds, and K. Laki. 1954. The amino acid composition of actin, myosin, tropomyosin and the meromyosins. *Arch. Biochem. Biophys.* 50:148–159.

Kostyuk, P. G., Z. A. Sorokina, and Yu. D. Kholodova. 1968. Measurement of activity of hydrogen, potassium and sodium ions in striated muscle fibers and nerve cells. *In* Intracellular Glass Microelectrodes. M. Lavallee, O. F. Schanne, and N. C. Herbert, editors. John Wiley & Sons, Inc., New York. 322–348.

Kushmerick, M. J., and R. J. Podolsky. 1969. Ionic mobility in muscle cells. *Science (Wash. DC)*. 166:1297–1298.

Lavallee, M. 1964. Intracellular pH of rat atrial muscle fibres measured by glass micropipette electrodes. *Circ. Res.* 15:185–193.

Lev, A. A. 1968. Electrochemical properties of so-called incompletely sealed cation sensitive microelectrodes. *In* Intracellular Glass Microelectrodes. M. Lavallee, O. F. Schanne, and N. C. Herbert, editors. John Wiley & Sons, Inc., New York. 76–94.

Magid, A., and M. Reedy. 1980. X-ray diffraction observations of chemically skinned frog skeletal muscle processed by an improved method. *Biophys. J.* 30:27–40.

McLachlan, A. D., and J. Karn. 1982. Periodic charge distributions in the myosin rod amino acid sequence match cross-bridge spacing in muscle. *Nature (Lond.)*. 299:226–231.

Matsubara, I., and G. F. Elliott. 1972. X-ray diffraction studies on skinned single fibers of frog skeletal muscle. *J. Mol. Biol.* 72:657–669.

Milhayi, E. 1950. The dissociation curves of crystalline myosin. *Enzymologica.* 14:224–236.

Millman, B. M., and B. G. Nickel. 1980. Electrostatic forces in muscle and cylindrical gel systems. *Biophys. J.* 32:49–63.

Naylor, G. R. S. 1977. X-ray and microelectrode studies of glycerinated rabbit psoas muscle. Ph.D. thesis, The Open University, Milton Keynes, England. 147 pp.

Naylor, G. R. S. 1978. A simple circuit for automatic continuous recording of microelectrode resistance. *Pfluegers Arch. Eur. J. Physiol.* 378:107–110.

Naylor, G. R. S. 1982. On the average electrostatic potential between the filaments in striated muscle and its relation to a simple Donnan potential. *Biophys. J.* 38:201–204.

Naylor W. G., and N. C. R. Merrellees. 1964. Some observations on the fine structure and metabolic activity of normal and glycerinated ventricular muscle of toad. *J. Cell. Biol.* 22:533–550.

Offer, G. 1973. C-protein — the periodicity in the thick filaments of vertebrate skeletal muscle. *Cold Spring Harbor Symp. Quant. Biol.* 37:87–93.

Pearlstone, J. R., P. Johnson, M. R. Carpenter, and L. R. Smillie. 1977. Primary structure of rabbit skeletal muscle troponin T. *J. Biol. Chem.* 252:983–989.

Pemrick, S. M., and C. Edwards. 1974. Differences in the charge distribution of glycerol extracted muscle fibers in rigor, relaxation, and contraction. *J. Gen. Physiol.* 64:551–567.

Pepe, F. H. 1967. The myosin filament 1. Structural organization from antibody staining observed in electron microscopy. *J. Mol. Biol.* 27:203–225.

Perrin, D. D., and I. G. Sayce. 1967. Computer calculation of equilibrium concentrations in mixtures of metal ions and complexing species. *Talanta.* 14:833–842.

Portzehl, H., P. C. Caldwell, and J. C. Ruegg. 1964. The dependence of contraction and relaxation of the muscle fibers from the crab Maio Squinado on the internal concentration of free calcium ions. *Biochem. Biophys. Acta.* 79:581–591.

Rashin A. A., and B. Honig. 1984. On the environment of ionizable groups in globular proteins. *Mol. Biol.* 173:515–521.

Rehm, W. S., M. Schwartz, and G. Carrasquer. 1984. Microelectrode artefact and the Donnan potential. *Biophys. J.* 45(2, Pt. 2):139*a* (Abstr.)

Rome, E. 1967. Light and x-ray diffraction studies of the filament lattice of glycerol-extracted rabbit psoas muscle. *J. Mol. Biol.* 27:591–602.

Rome, E. 1968. X-ray diffraction studies of the filament lattice of striated muscle in various bathing media. *J. Mol. Biol.* 37:331–344.

Sato, K. 1977. Modifications of glass microelectrodes: a self-filling and semi-floating microelectrode. *Am. J. Physiol.* 232:C207–C210.

Schanne, O. F., M. Lavallee, R. Laprade, and S. Gagne. 1968. Electrical properties of glass microelectrodes. *Proc. IEEE (Inst. Electr. Electron. Eng.)* 56:1072–1082.

Shapiro, P. J., K. Tawada, and R. J. Podolsky. 1979. X-ray diffraction of skinned muscle fibers. *Biophys. J.* 25:(2, Pt. 2):18*a*. (Abstr.)

Sillén, L. G., and A. E. Martell. 1964. Stability constants of metal-ion complexes. Special Publication No. 17, The Chemical Society, London.

Squire, J. M. 1973. General model of myosin filament structure. *J. Mol. Biol.* 77:291–323.

Stone, D., and L. B. Smillie. 1978. The amino acid sequence of rabbit skeletal α-tropomyosin. *J. Biol. Chem.* 253:1137–1148.

Szabo, G. 1966. Etude des phenomenes d'amplilfication ionique dans des membranes artificielles. Master's thesis, Universite de Montreal, Montreal, Canada.

Szent-Gyorgyi, A. 1949. Free-energy relations and contraction of actomyosin. *Biol. Bull. (Woods Hole).* 96:140–161.

Szent-Gyorgyi, A. 1951. The Chemistry of Muscular Contraction. Academic Press, Inc., New York. 162 pp.

Tasaki, K., Y. Tsukahara, and S. Ito. 1968. A simple, rapid and direct method for filling microelectrodes. *Physiol. Behav.* 3:1009–1010.

Teorell, T. 1953. Transport processes and electrical phenomena in ionic membranes. *Progr. Biophys.* 3:305–369.

Vieira, F. L., and M. I. Onuchic. 1978. Biological and artificial ion exchanges: Electrical measurements with glass microelectrodes. *Membr. Biol.* 40:157–164.

Weber, H. H., and H. Portzehl. 1952. Muscle contraction and fibrous muscle proteins. *Adv. Protein Chem.* 7:161–252.

Weber, H. H., and H. Portzehl. 1954. The transference of the muscle energy in the contraction cycle. *Prog. Biophys. Biophys Chem.* 4:60–111.

Weiss, R. M., R. Lazzara, and B. F. Hoffman. 1967. Potentials measured from glycerinated cardiac muscle. *Nature (Wash. DC).* 215:1305–1307.

White, D. C. S., and J. Thorson. 1972. Nonlinear dynamics of muscle. *J. Gen. Physiol.* 60:307–336.

Wilkinson, J. M., and R. J. A. Grand. 1975. Amino acid sequence of troponin I from rabbit skeletal muscle. *Biochem. J.* 149:493–496.